Chinese Journal of
POLYMER SCIENCE

RESEARCH ARTICLE

https://doi.org/10.1007/s10118-022-2658-8
Chinese J. Polym. Sci. **2022**, *40*, 567–575

Fractionated Crystallization Kinetics and Polymorphic Homocrystalline Structure of Poly($_L$-lactic acid)/Poly($_D$-lactic acid) Blends: Effect of Blend Ratio

Wang-Kai Xiang[a,b], Qing Xie[a], Shan-Shan Xu[a], Chen-Xuan Sun[a], Cheng-Tao Yu[a,b], Ying Zheng[a,b*], and Peng-Ju Pan[a,b*]

[a] *State Key Laboratory of Chemical Engineering, College of Chemical and Biological Engineering, Zhejiang University, Hangzhou 310027, China*
[b] *Institute of Zhejiang University-Quzhou, Quzhou 324000, China*

Abstract Stereocomplex (SC) crystallization has been an effective way to improve the physical performances of stereoregular polymers. However, the competition between homo and SC crystallizations can lead to more complicated crystallization kinetics and polymorphic crystalline structure in stereocomplexable polymers, which influences the physical properties of obtained materials. Herein, we select the medium-molecular-weight (MMW) poly($_L$-lactic acid)/poly($_D$-lactic acid) (PLLA/PDLA) asymmetric blends with different PDLA fractions (f_D=0.01–0.5) as the model system and investigate the effects of f_D and crystallization temperature (T_c) on the crystallization kinetics and polymorphic crystalline structure. We observe the fractionated (*i.e.*, multistep) crystallization kinetics and the formation of peculiar β-form homocrystals (HCs) in the asymmetric blends under quiescent conditions, which are strongly influenced by both f_D and T_c. Precisely, crystallization of β-form HCs is favorable in the MMW PLLA/PDLA blends with high f_D (≥0.2) at a low T_c (80–100 °C). It is proposed that the formation of metastable β-form HCs is attributed to the conformational matching between β-form HCs and SCs, and the stronger constrain effects of precedingly-formed SCs in the early stage of crystallization. Such effects can also cause the multistep crystallization kinetics of MMW PLLA/PDLA asymmetric blends in the heating process.

Keywords Poly(lactic acid); Stereocomplex crystallization; Polymorphic structure; Crystallization kinetics

Citation: Xiang, W. K.; Xie, Q.; Xu, S. S.; Sun, C. X.; Yu, C. T.; Zheng, Y.; Pan, P. J. Fractionated crystallization kinetics and polymorphic homocrystalline structure of poly($_L$-lactic acid)/poly($_D$-lactic acid) blends: effect of blend ratio. *Chinese J. Polym. Sci.* **2022**, *40*, 567–575.

INTRODUCTION

In the past few decades, poly(lactic acid) (PLA) derived from renewable resources has attracted great attention of both research and industry. PLA has been widely used to substitute the petroleum-based polymers,[1,2] due to its good biocompatibility, biodegradability, and processing ability.[3–5] Having two stereoisomers, poly($_L$-lactic acid) (PLLA) and poly($_D$-lactic acid) (PDLA), PLA can form stereocomplex (SC) crystals in its enantiomeric mixtures. In such crystalline phase, PLLA and PDLA chains are packed tightly by hydrogen-bonding interactions between the complementary enantiomeric chains.[6] Due to the unique crystalline structure, stereocomplexed PLA possesses better physical properties than the common homocrystalline one (*e.g.*, higher thermal and solvent resistances, mechanical properties, and gas barrier properties[7,8]). Thus, SC crystallization has been an effective way to enhance the physical properties of PLA-based materials.

Crystallization behavior of PLLA/PDLA blends is influenced by many variables such as molecular weight,[9–11] blend ratio,[12,13] polymer additives[14,15] and crystallization condition.[9,16] During crystallization, competitive crystallization between homocrystallites (HCs) and SCs are often observed in the PLLA/PDLA blends. Generally speaking, SCs can be exclusively obtained in the low-molecular-weight PLLA/PDLA blends (<~20 k),[9] which is much lower than that of commercialized PLA. When the molecular weight of PLLA/PDLA blend increases, the SC crystallization ability is gradually weakened. For instance, SCs and HCs form in comparable manner in the medium-molecular-weight (MMW, 20–50k) PLLA/PDLA blends. However, formation of SCs is obviously depressed and that of HCs becomes prevailing in the high-molecular-weight (HMW) PLLA/PDLA blends (>~50k). Therefore, elucidating the molecular-weight dependence of crystallization behavior of PLLA/PDLA blends is of fundamental importance to understand the SC crystallization mechanism.

Because of the competitive formations of HCs and SCs, crystallization kinetics and crystalline structure are more com-

* Corresponding authors, E-mail: yzheng1@zju.edu.cn (Y.Z.)
E-mail: panpengju@zju.edu.cn (P.J.P.)

Special Issue: Ordered Structure of Polymers
Received August 12, 2021; Accepted October 25, 2021; Published online January 11, 2022

plicated in the MMW and HMW PLLA/PDLA blends. As reported previously, MMW and HMW PLLA/PDLA blends undergo multistep crystallizations and the formation of SCs is more favorable in the initial stage of crystallization.[17,18] These precedingly-formed SCs could be regarded as physical cross-linkers that restrict the mobility of surrounding chains, which further influences the crystallization of PLLA/PDLA chains in the later homocrystallization process.[12,19–21] Previous studies reported that the precedingly-formed SCs lead to formation of unusual homocrystalline forms such as mesophase,[22] meta-form,[23] and modified HCs[24] in the PLLA/PDLA blends with specific molecular weights. Particularly, the precedingly-formed SCs was found to cause the fractionated crystallization kinetics and the formation of β-form HCs in the MMW PLLA/PDLA symmetric blend.[19] β-Form HC is a specific crystalline polymorph of homocrystalline PLLA and PDLA, which is generally obtained under rigorous crystallization conditions such as strong shearing or stretching under high pressure and temperature.[25–27]

Since PLLA and PDLA chains are alternately packed in the crystalline lattice of SCs,[28] blend ratio plays a key factor in the crystallization kinetics and crystalline structure of PLLA/PDLA blends. SCs are preferentially formed in PLLA/PDLA symmetric blend, but are highly suppressed when the PLLA/PDLA blend ratio is much deviated from 1:1.[13] The exceeded PLLA or PDLA would crystallize in HCs in the asymmetric PLLA/PDLA blends.[29,30] Accordingly, we anticipate that the blend ratio can strongly influence the fractionated crystallization kinetics and the formation of specific homocrystalline phase in the MMW PLLA/PDLA blend, which, however, remains unexplored in previous studies.

In this work, we choose MMW (~40k) PLLA/PDLA asymmetric blends with different PDLA fractions (f_D's, 0.01–0.5) as model samples, and investigate their crystallization kinetics and polymorphic crystalline structures in the crystallization process at various crystallization temperatures (T_c's, 70–140 °C). We illustrate the strong dependence of fractionated crystallization kinetics and homocrystalline structure of PLLA/PDLA blends on f_D and on T_c. In addition, we aim to present potential mechanisms of fractionated crystallization kinetics and β-form HC formation in asymmetric PLLA/PDLA blends.

EXPERIMENTAL

Materials and Sample Preparation

Both $_L$- and $_D$-lactide (optical purities >99.9%) were purchased from Purac Co., (Gorinchem, the Netherlands) and further purified by recrystallization from ethyl acetate. Tin (II) 2-ethylhexanoate [$Sn(Oct)_2$] and lauryl alcohol were purchased from Sigma-Aldrich Co., (St. Louis, MO, USA). MMW PLLA (M_w=41.1k, $Đ$=1.15) and PDLA (M_w=39.5 k, $Đ$=1.21) were synthesized by bulk ring-opening polymerization of lactide at 130 °C, with lauryl alcohol as initiator and $Sn(Oct)_2$ as catalyst.[19]

PLLA/PDLA blends were prepared through solution blending. PLLA and PDLA with different f_Ds (0.01–0.5) were separately dissolved in chloroform (50 g/L) and then mixed. The mixed solution was casted on a polytetrafluoroethylene dish and the solvent was evaporated at 25 °C for 24 h. Residual solvent was removed by further drying *in vacuo* at 80 °C for 6 h. For sake of clarity, the mass fraction of PDLA in PLLA/PDLA blends is denoted as f_D.

Characterizations

Differential scanning calorimetry (DSC)

DSC analysis was measured on a NETZSCH 214 Polyma DSC (NETZSCH, Germany) under a nitrogen gas flow (40 mL/min). The sample (8–10 mg) was melted at 260 °C and kept at this temperature for 3 min to erase the thermal history. For the nonisothermal cold crystallization, the sample was quenched into liquid nitrogen (denoted as melt-quenched sample), and then heated from 0 °C to 260 °C at 10 °C/min. For the isothermal crystallization, the sample was quickly cooled to 0 °C, then heated to the desire T_cs (70–140 °C) at 100 °C/min and held at this temperature for enough time to crystallize. Then, it was reheated to 260 °C at 10 °C/min to study the melting behavior.

Wide angle X-ray diffraction (WAXD)

WAXD measurements of isothermally-crystallized PLLA/PDLA blends were carried out on the beamline BL16B1 of Shanghai Synchrotron Radiation Facility (SSRF). The wavelength of X-ray is 0.124 nm. Diffraction patterns were collected using a Rayonix SX-165 CCD detector (Rayonix Illinois, USA). The crystallized samples used for WAXD measurement were treated by the same thermal procedure as those for DSC analysis. The sample-to-detector distance of WAXD measurement was 155 mm and the acquisition time of each WAXD pattern was 30 s. For temperature-variable WAXD measurements, the melt-quenched sample was sandwiched by polyimide films and heated from 40 °C to 260 °C on a Linkam THMS600 hot stage (Linkam Scientific Instrument Ltd., Surrey, UK) at 10 °C/min. The pattern was collected with a temperature interval of 5 °C and an acquisition time of 15 s. 2D-WAXD data were converted into 1D pattern by integration with a Fit2D software.

Overall crystallinity (X_{total}) and crystallinities of SCs (X_{SC}), β-HCs (X_β), $\alpha(\alpha')$-HCs [$X_{\alpha(\alpha')}$] of PLLA/PDLA blends were evaluated from the WAXD patterns with a X'Pert HighScore software.[31] X_{total} was estimated by comparing the area of total diffractogram with the area of Bragg reflections after subtracting the amorphous halo; X_{SC}, $X_{\alpha(\alpha')}$ and X_β were calculated from the diffraction peak area obtained by peak splitting/fitting:[32]

$$X_{SC} = \frac{A_{SC}}{A_{SC} + A_{\alpha(\alpha')} + A_\beta} X_{total} \quad (1)$$

$$X_{\alpha(\alpha')} = \frac{A_{\alpha(\alpha')}}{A_{SC} + A_{\alpha(\alpha')} + A_\beta} X_{total} \quad (2)$$

$$X_\beta = \frac{A_\beta}{A_{SC} + A_{\alpha(\alpha')} + A_\beta} X_{total} \quad (3)$$

where A_{SC}, $A_{\alpha(\alpha')}$, and A_β correspond to the diffraction peak areas of SCs, $\alpha(\alpha')$- and β-HCs, respectively.

RESULTS AND DISCUSSION

Nonisothermal Crystallization Kinetics

Nonisothermal crystallization kinetics of PLLA/PDLA blends with different f_Ds (0.01–0.5) were investigated by DSC. Fig. 1 depicts the DSC heating curves of melt-quenched blends with different f_Ds at 10 °C/min. Obviously, the crystallization and melting behaviors of PLLA/PDLA blends are highly dependent on f_D. The blend with f_D=0.01 exhibits a sharp cold crystallization peak (P_{c1})

https://doi.org/10.1007/s10118-022-2658-8

at 94 °C and a broad melting region at 140–190 °C, indicating the formation of HCs during heating. However, the blends with f_D=0.1–0.5 show two melting regions at temperature ranges of 150–180 and 200–250 °C, corresponding to the melts of HCs and SCs, respectively. The formation of SCs is favorable and that of HCs is substantially suppressed when f_D is close to 0.5. Melting enthalpy of SCs ($\Delta H_{m,SC}$) increases and that of HCs ($\Delta H_{m,HC}$) decreases with increasing the f_D. Since PLLA and PDLA chains are alternatively packed in the crystalline lattice of SCs,[28] SCs are preferentially generated when the PLLA and PDLA fractions are equivalent. Moreover, the blends with high f_D (≥0.2) exhibit dual melting peaks (P_{m1}, P_{m2}) in the melting region of SCs, originating from the melt-recrystallization mechanism.[9]

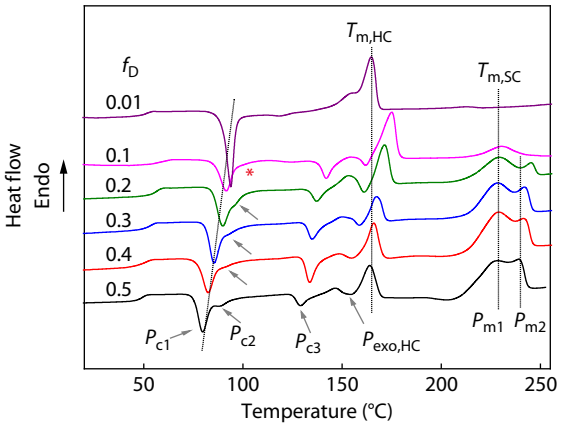

Fig. 1 DSC heating curves of melt-quenched PLLA/PDLA blends with different f_Ds.

The blends with high f_D exhibit multiple exotherm peaks (P_{c1}, P_{c2}, P_{c3}) and an exotherm peak ($P_{exo,HC}$) prior to the dominant melting peak of HCs. P_{c1} and P_{c3} are well separated and P_{c2} seems to be a shoulder or tail of P_{c1}. The appearance of $P_{exo,HC}$ stems from the heating-induced structural transition (*i.e.*, *β*-to-*α* crystal transition) of HCs in the heating process.[19] The multiple exotherm peaks (P_{c1}, P_{c2}, P_{c3}) shift to lower temperature with increasing f_D from 0.1 to 0.5, implying the accelerated crystallization at higher f_D. P_{c2} becomes less visible as f_D decreases from 0.5 to 0.1 and nearly diminishes in the blend with f_D=0.1 (indicated by the red asterisk). Since the PLLA and PDLA used have similar molecular weights (~40k) and crystallization rates, the observation of multiple exotherm peaks in asymmetric PLLA/PDLA blends could be ascribed to the fractionated formation of different crystals.[33] Fractionated crystallizations are usually reported in block polymers[34–36] and polymer blends[37,38] that are phase-separated in the nanometer scale. The mechanism of fractionated crystallization for melt-quenched blends will be discussed in the following part with the combination of temperature-variable WAXD results.

Melting Behavior and Crystalline Structure

We studied the melting behavior and crystalline structure of PLLA/PDLA blends after isothermal crystallization at different T_cs. Melting behavior and crystalline structures of the blends depend strongly on f_D. Figs. 2(a) and 2(b) show the DSC heating curves of the blends with f_D=0.01–0.5 after isothermal crystallization at T_c=90 and 120 °C. As shown in Fig. 2(a), although the blends with various f_Ds were crystallized at T_c= 90 °C for enough time, a cold crystallization peak (P_{c3}) can still be observed at 125–145 °C upon subsequent heating. This suggested that the blends with f_D=0.1–0.5 did not crystallize completely after annealing at T_c=90 °C. The exothermic peak ($P_{exo,HC}$) related to the structural transition of HCs is also observed before the melting peak of HCs for the blends with f_D=0.1–0.5. However, the exothermic peaks of P_{c3} and $P_{exo,HC}$ are absent for the blends crystallized at a high T_c of 120 °C (Fig. 2b), indicating the sufficient crystallization and the formation of stable crystals under this condition.

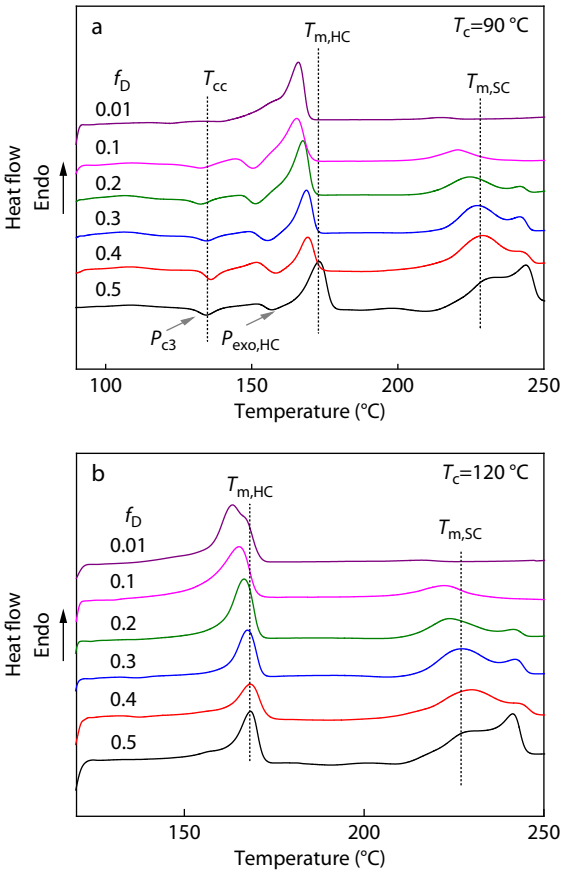

Fig. 2 DSC heating curves of PLLA/PDLA blends with different f_Ds after isothermal crystallization at (a) 90 °C and (b) 120 °C. The heating rate is 10 °C/min.

As seen in Figs. 2(a) and 2(b), the blends crystallized at T_c=90 and 120 °C exhibit the melting region of HCs at 150–175 °C and that of SCs at 210–245 °C. The blends with high f_Ds (≥0.2) display dual melting peaks of SCs at 210–245 °C, due to the melt recrystallization mechanism.[19] Melting temperatures of HCs ($T_{m,HC}$) and SCs ($T_{m,SC}$) increase from 167 °C to 169 °C and from 224 °C to 228 °C respectively, as f_D increases from 0.1 to 0.5, which is ascribed to the formation of more ordered crystals in the blends with high f_D.

Figs. 3(a) and 3(b) show the corresponding WAXD patterns of PLLA/PDLA blends with different f_Ds crystallized at T_c=90 and 120 °C. Crystalline polymorphs of the blends are influenced not only by f_D, but also by T_c. Characteristic diffraction

https://doi.org/10.1007/s10118-022-2658-8

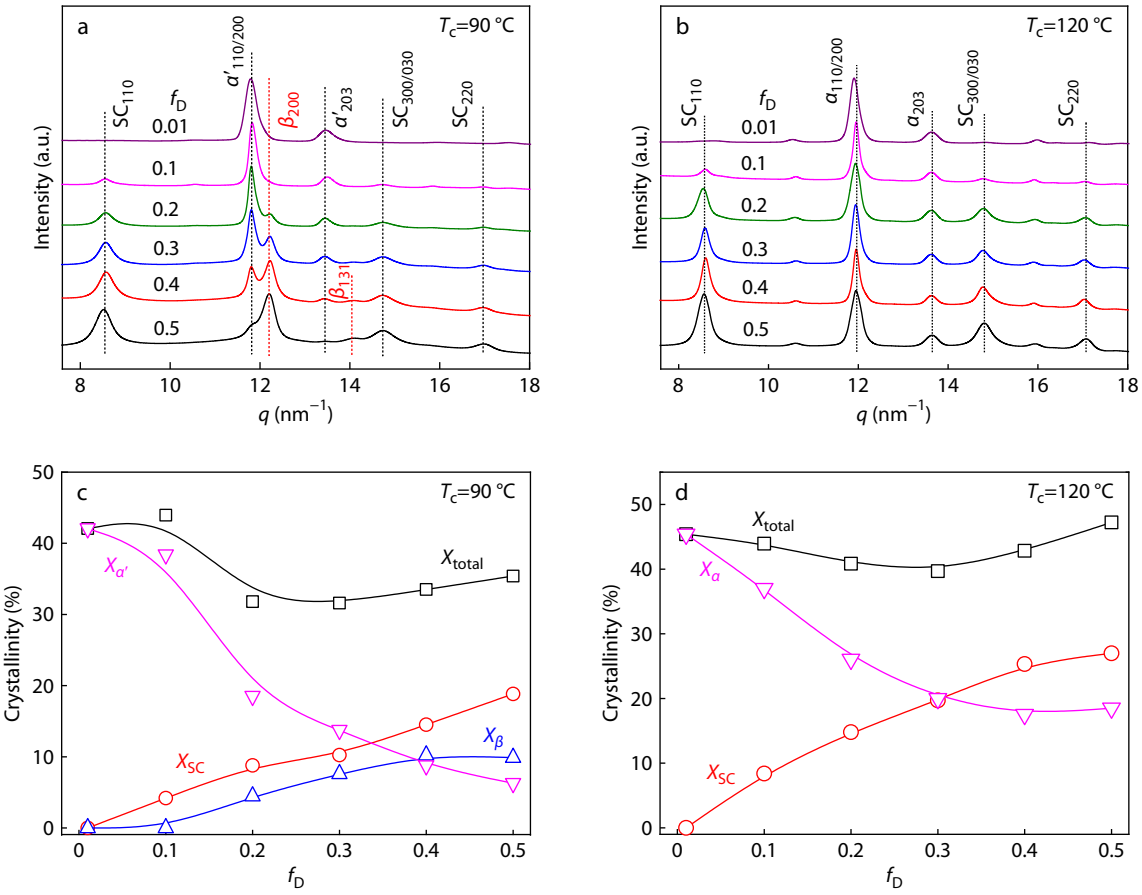

Fig. 3 WAXD results of PLLA/PDLA blends after isothermal crystallization at 90 and 120 °C: WAXD patterns for the samples crystallized at (a) 90 °C and (b) at 120 °C; (c) Plots of α'-HC, β-HC, SC and total crystallinities as a function of f_D for the samples crystallized at 90 °C; (d) plots of α-HC, SC and total crystallinities as a function of f_D for the samples crystallized at 120 °C.

peaks located at q=11.7 and 13.4 nm^{-1} are observed for the blend with f_D=0.01 (Fig. 3a), which are assigned to the (110)/(200) and (203) planes of α'-form HCs, respectively.[39] The characteristic diffraction peaks located at q=8.5, 14.7, and 17.0 nm^{-1} appear for the blend with f_D=0.1, which are attributed to (110), (300)/(030) and (220) planes of SCs, respectively.[40] Two new diffraction peaks located at q=12.2 and 14.0 nm^{-1} are observed in the WAXD pattern as f_D increases to 0.2–0.5, besides the diffraction peaks of α'-HCs and SCs. In order to clarify the crystalline polymorph, we enlarged WAXD pattern of the blends with f_D=0.4 crystallized at 90 °C from Fig. 3(a), as shown in Fig. 4. In addition to the diffraction peaks of α'-form HCs and SCs, the other diffraction peaks located at q=12.2, 14.0, 15.8, 18.5, 19.9, 21.0, and 22.5 nm^{-1} (d=0.517, 0.448, 0.397, 0.339, 0.315, 0.298, and 0.279 nm) correspond to the (200), (131), (221), (132), (222), (003), and (023) planes of β-form HCs, respectively.[41] As shown in Fig. 3(a), the peak intensities of SCs and β-HCs are enhanced but those of α'-form HCs decrease as f_D increases from 0.2 to 0.5, demonstrating that similar amounts of PLLA to PDLA are favorable for the formation of β-HCs in the blend.

On basis of the WAXD results, X_{total}, $X_{\alpha'}$, X_{SC}, and X_β values are quantitatively evaluated and plotted as a function of f_D in Fig. 3(c). X_{total}, $X_{\alpha'}$, X_{SC}, and X_β show quite different variation tendencies with f_D in the blends. The blend with f_D=0.01 crystallizes solely in α'-form HCs with the $X_{\alpha'}$ value of 42.1%. $X_{\alpha'}$ value drops from 38.4% to 18.5% and the SCs and β-form HCs are formed as f_D enhances from 0.1 to 0.2. Notably, X_β and X_{SC} in the blend show similar f_D-dependent evolutions in the blend with f_D=0.2–0.5. X_β and X_{SC} increase from 4.5% to 9.9% and from 8.8% to 18.8%, respectively, as f_D varies from 0.2 to 0.5. Accordingly, we consider that formation of β-HCs is re-

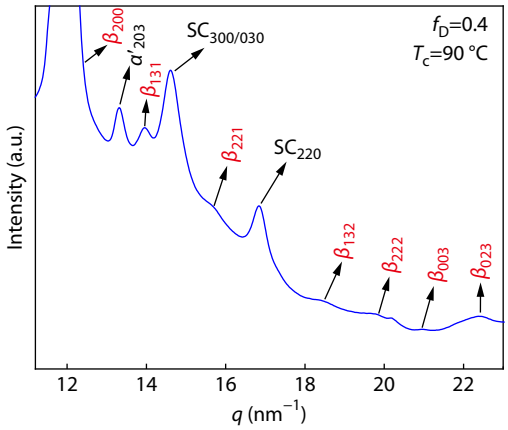

Fig. 4 Enlarged WAXD pattern of the blends with f_D=0.4 crystallized at 90 °C.

https://doi.org/10.1007/s10118-022-2658-8

lated to the existence of SCs, as will be explained in the following section. Additionally, formation of α'-HCs is competitive with that of the SCs and β-HCs, resulting in a minimum X_{total} value of 31.7% in the blend with f_D=0.3.

We further studied the polymorphic crystalline structures of the blends crystallized at a high T_c. Fig. 3(b) shows the WAXD patterns of the blends with different f_Ds after crystallization at T_c=120 °C. The α-HCs and SCs are predominantly formed in the blends at a high T_c of 120 °C. As shown in Fig. 3(b), characteristic diffraction peaks of α-HCs (q=11.9 and 13.6 nm^{-1}, (110/200) and (203) planes of α-HCs) and SCs (q=8.5, 14.7, and 17.0 nm^{-1}, (110), (300/030) and (220) plane of SCs) are present, while the diffraction peaks of β-HCs (q=12.2 and 14.0 nm^{-1}, (200) and (131) planes of β-HCs) are absent for the blends with f_D=0.01–0.5 after crystallization at T_c=120 °C. Fig. 3(d) shows the variations of X_{total}, X_α, and X_{sc} with f_D for the blend crystallized at T_c=120 °C. X_α value decreases from 45.4% to 18.0% and X_{sc} value increases from 0% to 27.0% at T_c=120 °C as f_D varies from 0.01 to 0.5. Similar to the blends crystallized at T_c=90 °C, competitive crystallization of HCs and SCs results in a minimum X_{total} value of 40.0% in the blend with f_D=0.3. Therefore, we conclude that β-HCs are predominantly formed in the blends with a high f_D (≥0.2) at a low T_c (*e.g.*, 90 °C).

To further elucidate the effect of T_c on polymorphic structure, we investigate the crystalline structure of the blends with various f_Ds (0.1–0.4) that are crystallized at different T_cs (70–140 °C). Fig. 5 shows the WAXD patterns of the blends with f_D=0.1–0.4 crystallized at T_c=70–140 °C. As expected, β-HCs are generated in the blends with a high f_D (0.2–0.4) but not in those with a low f_D (0.1). Fig. 5(a) shows that the blend with f_D = 0.1 crystallizes in SCs+α'-HCs and SCs+α-HCs mixtures at T_c≤100 °C and ≥110 °C, respectively. The blend with f_D=0.2 crystallizes in SCs+α'-HCs+β-HCs and SCs+α-HCs mixtures at T_c≤100 °C and ≥110 °C, respectively (Fig. 5b). The blends with f_D=0.3–0.4 (Figs. 5c and 5d) have similar f_D-dependence of crystalline polymorphs to the blend with f_D=0.2. We note that the (200) diffraction intensity of β-HCs increases remarkably as f_D enhances from 0.2 to 0.4. β-HC shows the highest diffraction intensity at T_c=90 °C for the blends with f_D=0.2–0.4, indicating that the formation of β-HC is preferable at medium T_c.

Fig. 6 depicts the X_{SC}, X_β, $X_{\alpha(\alpha')}$, and X_{total} of the blends with f_D=0.2 and 0.4 after isothermal crystallization at various T_cs. These blends exhibit similar variation trends for each crystalline polymorph fraction with T_c. Fig. 6 shows that X_{total}, X_{sc}, and $X_{\alpha(\alpha')}$ increase gradually with enhancing T_c from 80 °C to 120 °C and then remain nearly unchanged as T_c further increases to 140 °C, which indicates that the crystallization of blend is constrained at a low T_c (<110 °C). In case of the blends with f_D=0.2 and 0.4, X_β enhances slightly from 4.0% to 4.5% and from 9.4% to 10.2% with increasing T_c from 80 °C to 90 °C, and then decreases to zero with further increasing T_c to above 100 °C. β-HCs are favored at a medium T_c and in the

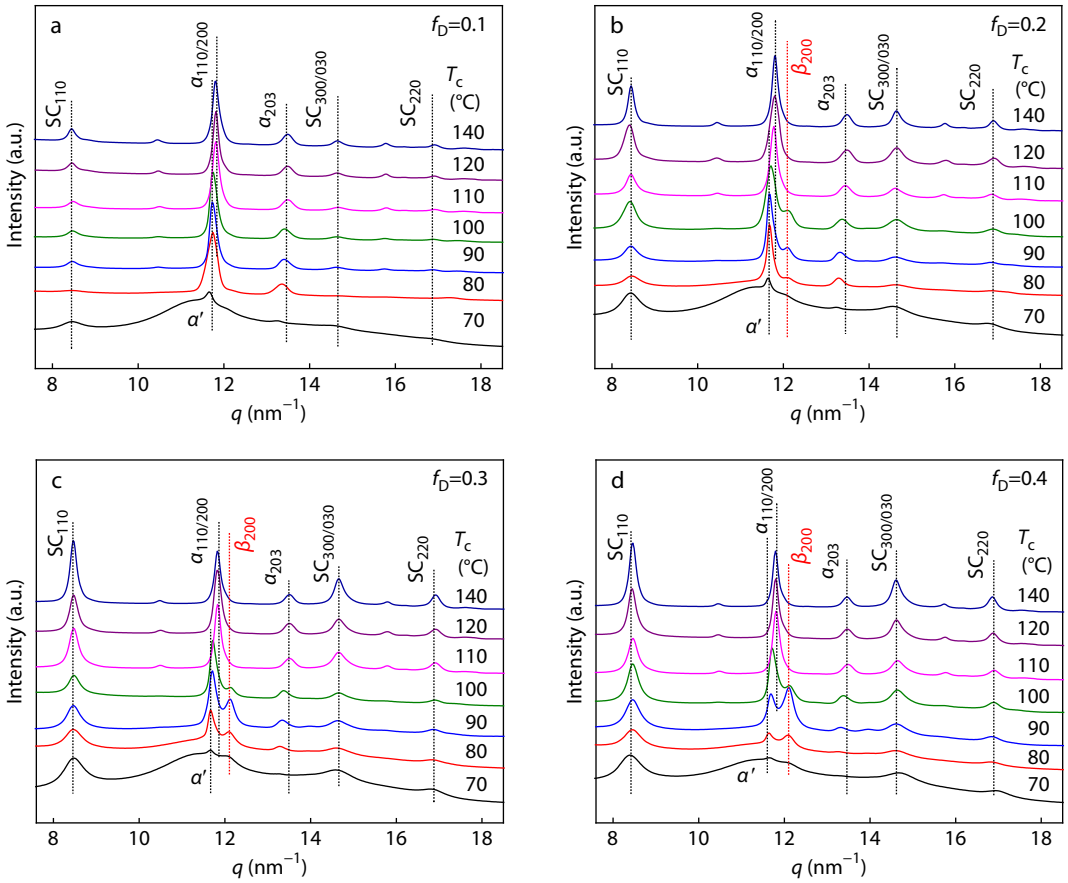

Fig. 5 WAXD patterns of PLLA/PDLA blends after isothermal crystallization at various T_cs: (a) f_D=0.1; (b) f_D=0.2; (c) f_D=0.3; (d) f_D=0.4.

https://doi.org/10.1007/s10118-022-2658-8

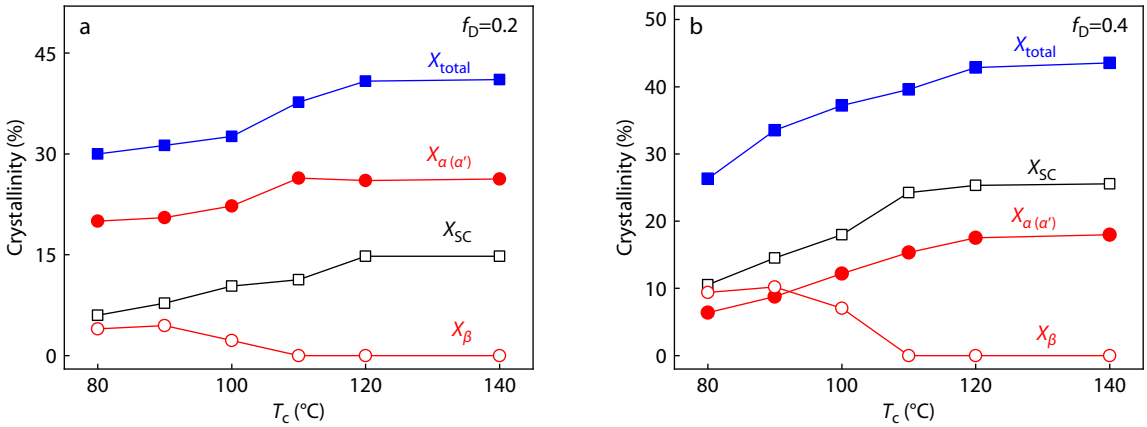

Fig. 6 Plots of $\alpha(\alpha')$-HC, β-HC, SC and total crystallinities as a function of T_c for the PLLA/PDLA blends after isothermal crystallization at various T_cs: (a) f_D=0.2; (b) f_D=0.4.

blends with comparable PLLA and PDLA fractions. The blends with f_D=0.2 and 0.4 show maximum X_β values of 4.5% and 10.2% at T_c=90 °C.

On basis of the WAXD results, we summarized the T_c and f_D-dependent polymorphic crystalline structure of PLLA/PDLA blends in Fig. 7. Crystalline polymorphs of the blends show strong dependences on both f_D and T_c. As shown in Fig. 7, the asymmetric blends crystallize in SCs+α-HCs mixture at a high T_c (≥110 °C), regardless of the f_D. However, the blends with the low (≤0.1) and high (≥0.2) f_Ds crystallize in SCs+α'-HCs and SCs+α'-HCs+β-HCs mixtures at a low T_c (≤100 °C), respectively.

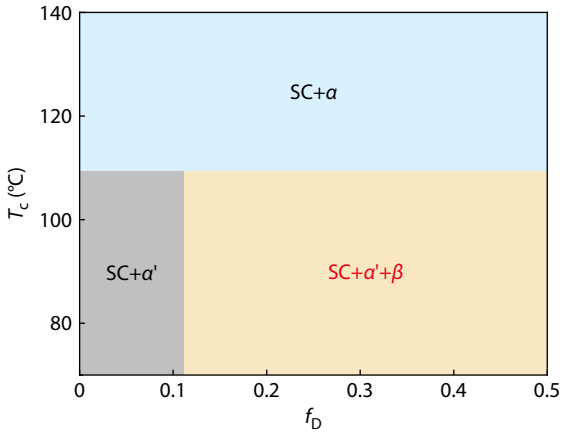

Fig. 7 Phase diagram of PLLA/PDLA blends with different f_Ds crystallized at various T_cs.

As mentioned above, β-HCs are preferentially generated in the blends with a high f_D (≥0.2) at a low T_c (≤100 °C). In order to quantitatively analyze the crystallization kinetics, we chose the blends with a low (0.01) and a high (0.3) f_Ds as model samples and calculated the crystallization half-time ($t_{0.5}$) and Avrami index (n) from the DSC curves collected in isothermal crystallization at a low T_c (70–100 °C) by Avrami equation.[42] Fig. 8 shows the inverse $t_{0.5}$ ($1/t_{0.5}$) and n values of the blends isothermally-crystallized at a low T_c (70–100 °C). Fig. 8(a) shows that $1/t_{0.5}$ value increases gradually as T_c varies from 70 °C to 100 °C, indicating the faster crystallization at a higher T_c;

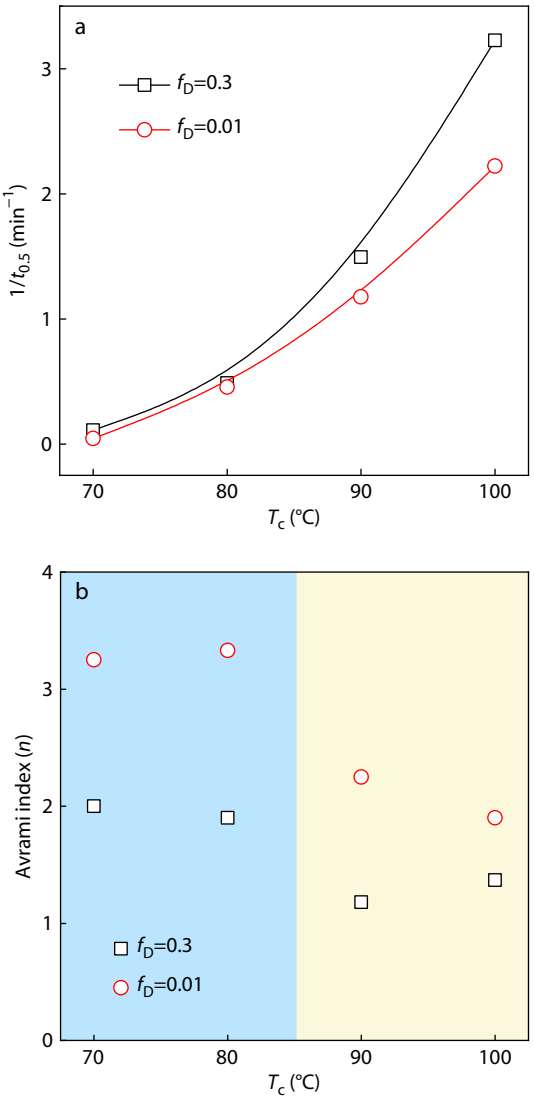

Fig. 8 Kinetic parameters of PLLA/PDLA blends after isothermal crystallization at low T_cs (70–100 °C): (a) $1/t_{0.5}$ versus T_c; (b) Avrami index (n) versus T_c.

https://doi.org/10.1007/s10118-022-2658-8

this is due to the enhanced diffusion ability and mobility of PLLA/PDLA chains at a higher T_c. In addition, crystallization of the blends becomes faster with increasing f_D from 0.01 to 0.3 at the same T_c, due to the heterogeneous nucleation effect of pre-formed SCs on following homocrystallization.[43] Fig. 8(b) shows that the blend with f_D=0.01 has the n values of 2–3 at a low T_c (70–100 °C). However, the blend with f_D=0.3 has the n values of ~2 at T_c=70–80 °C but ~1 at T_c=90–100 °C. Governed by the crystal growth geometry and time dependence of nucleation,[44] the n value is generally around 2–4 for semicrystalline polymers in common crystallization processes. First-order crystallization kinetics (n=1) are frequently found in the confined crystallization of polymers.[44–46] Therefore, the small n value for the blends (*e.g.*, f_D=0.3) at T_c=90–100 °C suggests the occurrence of constrained crystallization.

Proposed Mechanisms for Fractionated Crystallization and β-HC Formation

In order to clarify the fractionated crystallization mechanism, crystallization and structural evolution of melt-quenched asymmetric blends with different f_D's (0.1–0.4) were investigated by *in situ* WAXD upon heating (Fig. 9). As shown in Fig. 9(a), the melt-quenched blend with f_D=0.4 is amorphous at temperature below 60 °C. SCs start to crystallize with heating to 60–80 °C, resulting in the appearance of P_{c1} in Fig. 1. β-HCs are present with further heating to 110–120 °C, leading to the appearance of P_{c2} in Fig. 1. Diffractions of SCs and β-HCs become remarkable at 120–140 °C, which corresponds to the temperature range of P_{c3} (Fig. 1). β-HCs are metastable and transform into the thermodynamically stable α-HCs with further heating to 150–160 °C; this temperature range agrees with that of $P_{exo,HC}$ (Fig. 1). HCs melt first and then SCs melt with further heating to 250 °C. Similar sequential crystallization and β-to-α phase transition are also observed in the melt-quenched blend with f_D=0.2 upon heating (Fig. 9b). Based on both DSC and WAXD data, we conclude that the multiple crystallization peaks (P_{c1}, P_{c2}, P_{c3}) observed upon heating for melt-quenched blends with f_D=0.2–0.5 should stem from the crystallization of SCs (P_{c1}), crystallization of β-HCs (P_{c2}), and further crystallization of β-HCs and SCs (P_{c3}), respectively. $P_{exo,HC}$ observed in the DSC heating curves of melt-quenched blends with f_D=0.2–0.5 is attributed to the heating-induced β-to-α phase transition. Previous study has demonstrated that the heating-induced β-to-α transition proceeds through melt-recrystallization route, rather than the direct solid-to-solid route.[19] The blend with a low f_D (*e.g.*, 0.1) crystallizes directly in α-HCs at 110–120 °C, without forming β-HCs (Fig. 9c). The P_{c1} and P_{c3} observed in Fig. 1 for the blend with f_D=0.1 correspond to the crystallization of SCs (P_{c1}), and further crystallization of SCs and α-HCs (P_{c3}).

β-Form HC is a special polymorph of homocrystalline PLLA and PDLA, which is usually obtained under rigorous crystallization conditions such as high pressure, strong stretching or shearing.[28] Herein, β-HCs can be obtained in the MMW PLLA/PDLA blends with a high f_D (≥0.2) under mild conditions such as at a low T_c (80–100 °C), without employing the pressure, shearing or stretching. We propose that the formation of β-HCs is ascribed to (i) the conformational matching between SCs and β-HCs, and (ii) the constrained effects of pre-formed SCs. Due to the conformational similarity of β-HCs to that of SCs (3_1 helix conformation),[25,47] PLLA and PDLA

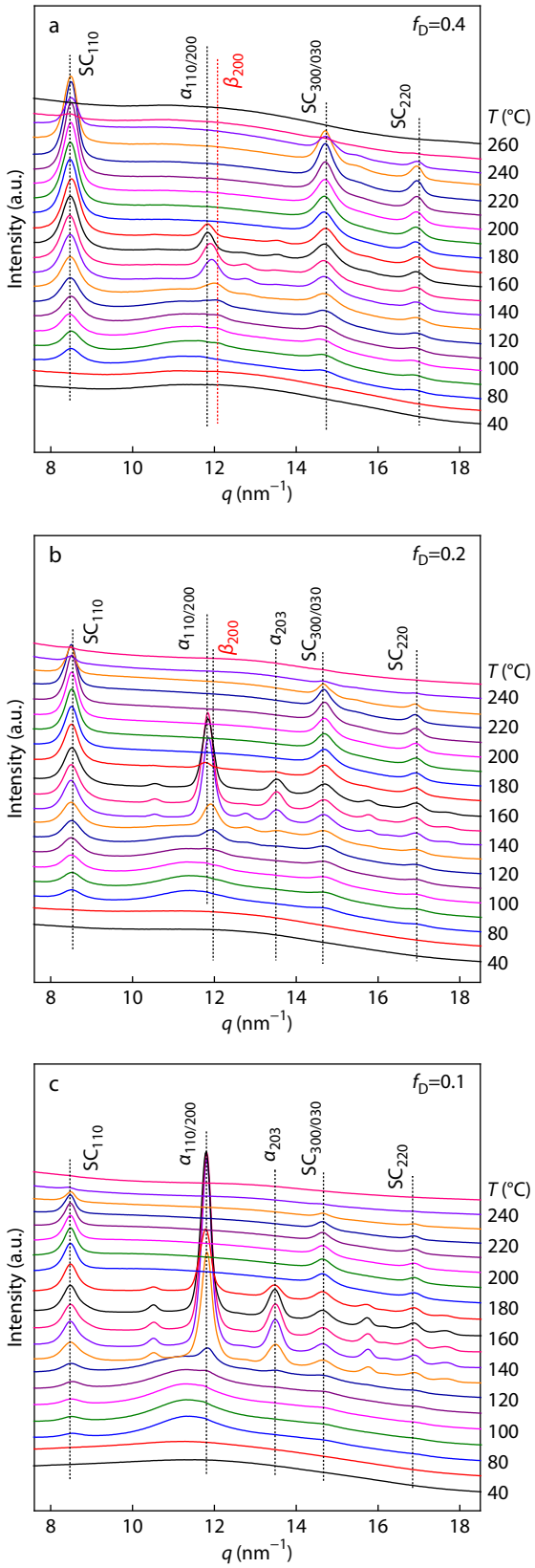

Fig. 9 Temperature-dependent WAXD patterns of melt-quenched PLLA/PDLA blends collected upon heating at 10 °C/min: (a) f_D=0.4; (b) f_D=0.2; (c) f_D=0.1.

https://doi.org/10.1007/s10118-022-2658-8

chains would prefer the formation of β-HCs to the conventional $\alpha(\alpha')$-HCs adopting 10_3 helix conformation.[41] On the other hand, the MMW blends with high f_D show stronger constrained effects at low T_c=90–100 °C, as demonstrated by n=~1 in Fig. 8(b). Temperature-variable WAXD results (Fig. 9) have revealed that SCs are formed prior to HCs in the crystallization process. The precedingly-crystallized SCs in the early stage can act as physical crosslinkers and form physical networks in the PLLA/PDLA matrix, which would restrict the diffusion of surrounding chains and thus constrain the following crystallization of PLLA and PDLA. Therefore, it would be easier for PLLA and PDLA to crystallize in the β-HCs adopting more extended conformation. Moreover, such constrained effect by formation of SCs becomes more predominant at a high fraction of SCs. As a result, β-HCs are only crystallized in the MMW PLLA/PDLA blends with a high f_D (≥0.2), but not in the blends with a low f_D (≤0.1). Finally, at high T_cs (≥110 °C), the blends would prefer to crystallize in conventional α-HCs for that the mobility of PLLA and PDLA chains increase at small supercooling.

CONCLUSIONS

In summary, we have elucidated the multistep crystallization kinetics and polymorphic crystalline structures of MMW PLLA/PDLA asymmetric blends with different f_Ds (0.01–0.5) under various crystallization conditions. Crystallization kinetics and crystalline structure of PLLA/PDLA asymmetric blends depend on f_D and T_c. The asymmetric PLLA/PDLA blends with a high f_D (≥0.2) show fractionated crystallization kinetics and form peculiar β-form HCs when being crystallized at a low T_c (80–100 °C), while the blends crystallize into the usual α-form HCs and SCs at a higher T_c (≥110 °C). We propose that the fractionated crystallization kinetics of MMW PLLA/PDLA asymmetric blends are originated from the constrained effects of pre-formed SCs. Formation of metastable β-form HCs is probably attributed to the conformational matching between β-form HCs and SCs, and also to the stronger constrained effects by precedingly-formed SCs in the early stage of crystallization. This work has shed light on the complicated crystallization kinetics and polymorphic structure of stereocomplexable polymers and put forward potential methods to tune the crystalline structure of stereocomplexed materials.

NOTES

The authors declare no competing financial interest.

ACKNOWLEDGMENTS

This study was financially supported by the National Natural Science Foundation of China (No. 21873083). WAXD measurement were performed on the beamline BL16B1 of SSRF.

REFERENCES

1 Auras, R.; Harte, B.; Selke, S. An overview of polylactides as packaging materials. *Macromol. Biosci.* **2004**, *4*, 835–64.
2 Lassalle, V.; Ferreira, M. L. PLA nano- and microparticles for drug delivery: an overview of the methods of preparation. *Macromol. Biosci.* **2007**, *7*, 767–783.
3 Zhu, Y.; Romain, C.; Williams, C. K. Sustainable polymers from renewable resources. *Nature* **2016**, *540*, 354–362.
4 Zheng, Y.; Zhang, C.; Bao, Y.; Shan, G.; Pan, P. Temperature-dependent crystallization and phase transition of poly(L-lactic acid)/CO_2 complex crystals. *Chinese J. Polym. Sci.* **2021**, *39*, 484–492.
5 Rocca-Smith, J. R.; Pasquarelli, R.; Lagorce-Tachon, A.; Rousseau, J.; Fontaine, S.; Aguié-Béghin, V.; Debeaufort, F.; Karbowiak, T. Toward sustainable PLA-based multilayer complexes with improved barrier properties. *ACS Sustain. Chem. Eng.* **2019**, *7*, 3759–3771.
6 Pan, P.; Yang, J.; Shan, G.; Bao, Y.; Weng, Z.; Cao, A.; Yazawa, K.; Inoue, Y. Temperature-variable FTIR and solid-state ^{13}C NMR investigations on crystalline structure and molecular dynamics of polymorphic poly(L-lactide) and poly(L-lactide)/poly(D-lactide) stereocomplex. *Macromolecules* **2012**, *45*, 189–197.
7 Tsuji, H. Poly(lactic acid) stereocomplexes: a decade of progress. *Adv. Drug Deliv. Rev.* **2016**, *107*, 97–135.
8 Liu, G.; Zhang, X.; Wang, D. Tailoring crystallization: towards high-performance poly(lactic acid). *Adv. Mater.* **2014**, *26*, 6905–6911.
9 Pan, P.; Han, L.; Bao, J.; Xie, Q.; Shan, G.; Bao, Y. Competitive stereocomplexation, homocrystallization, and polymorphic crystalline transition in poly(L-lactic acid)/poly(D-lactic acid) racemic blends: molecular weight effects. *J. Phys. Chem. B* **2015**, *119*, 6462–6470.
10 Pan, P.; Kai, W.; Zhu, B. Polymorphous crystallization and multiple melting behavior of poly(L-lactide): molecular weight dependence. *Macromolecules* **2007**, *40*, 6898–6905.
11 Hu, D.; Chen, M.; Yang, Y.; Li, H. Texture induced by molecular weight dispersity: polymorphism within poly(L-lactic acid) spherulites. *Chinese J. Polym. Sci.* **2020**, *38*, 1365–1373.
12 Wei, X.; Bao, R.; Cao, Z.; Yang, W.; Xie, B.; Yang, M. Stereocomplex crystallite network in asymmetric PLLA/PDLA blends: formation, structure, and confining effect on the crystallization rate of homocrystallites. *Macromolecules* **2014**, *47*, 1439–1448.
13 Tsuji, H.; Ikada, Y. Stereocomplex formation between enantiomeric poly(lactic acids). 9. Stereocomplexation from the melt. *Macromolecules* **1993**, *26*, 6918–6926.
14 Ju, Y.; Li, X.; Diao, X.; Bai, H.; Zhang, Q.; Fu, Q. Mixing of racemic poly(L-lactide)/poly(D-lactide) blend with miscible poly(D,L-lactide): toward all stereocomplex-type polylactide with strikingly enhanced SC crystallizability. *Chinese J. Polym. Sci.* DOI: 10.1007/s10118-021-2588-x.
15 Bao, R.; Yang, W.; Wei, X.; Xie, B.; Yang, M. Enhanced formation of stereocomplex crystallites of high molecular weight poly(L-lactide)/poly(D-lactide) blends from melt by using poly(ethylene glycol). *ACS Sustain. Chem. Eng.* **2014**, *2*, 2301–2309.
16 Bao, R.; Yang, W.; Jiang, W.; Liu, Z.; Xie, B.; Yang, M. Polymorphism of racemic poly(L-lactide)/poly(D-lactide) blend: effect of melt and cold crystallization. *J. Phys. Chem. B* **2013**, *117*, 3667–3674.
17 Hu, J.; Wang, J.; Wang, M.; Ozaki, Y.; Sato, H.; Zhang, J. Investigation of crystallization behavior of asymmetric PLLA/PDLA blend using Raman Imaging measurement. *Polymer* **2019**, *172*, 1–6.
18 Henmi, K.; Sato, H.; Matsuba, G.; Tsuji. H.; Nishida, K.; Kanaya, T.; Oda, A.; Endou, K. Isothermal crystallization process of poly(L-lactic acid)/poly(D-lactic acid) blends after rapid cooling from the melt. *ACS Omega* **2016**, *1*, 476–482.
19 Xie, Q.; Bao, J.; Shan, G.; Bao, Y.; Pan, P. Fractional crystallization kinetics and formation of metastable β-form homocrystals in poly(L-lactic acid)/poly(D-lactic acid) racemic blends induced by precedingly formed stereocomplexes. *Macromolecules* **2019**, *52*, 4655–4665.
20 Saeidlou, S.; Huneault, M. A.; Li, H.; Sammut, P.; Park, C. B.

Evidence of a dual network/spherulitic crystalline morphology in PLA stereocomplexes. *Polymer* **2012**, *53*, 5816–5824.
21 Xie, Q.; Guo, G.; Lu, W.; Sun, C.; Zhou, J.; Zheng, Y.; Shan, G.; Bao, Y.; Pan, P. Polymorphic homocrystallization and phase behavior of high-molecular-weight poly(L-lactic acid)/poly(D-lactic acid) racemic mixture with intentionally enhanced stereocomplexation ability *via* miscible blending. *Polymer* **2020**, *201*, 122597.
22 Yang, C.; Huang, Y.; Ruan, J.; Su, A. Extensive development of precursory helical pairs prior to formation of stereocomplex crystals in racemic polylactide melt mixture. *Macromolecules* **2012**, *45*, 872–878.
23 Chang, L.; Woo, E. M. A unique meta-form structure in the stereocomplex of poly(D-lactic acid) with low-molecular-weight poly(L-lactic acid). *Macromol. Chem. Phys.* **2011**, *212*, 125–133.
24 Shao, J.; Sun, J.; Bian, X.; Cui, Y.; Zhou, Y.; Li, G.; Chen, X. Modified PLA homochiral crystallites facilitated by the confinement of PLA stereocomplexes. *Macromolecules* **2013**, *46*, 6963–6971.
25 Ru, J.; Yang, S.; Zhou, D.; Yin, H.; Lei, J.; Li, Z. Dominant β-form of poly(L-lactic acid) obtained directly from melt under shear and pressure fields. *Macromolecules* **2016**, *49*, 3826–3837.
26 Sawai, D.; Takahashi, K.; Sasashige, A.; Kanamoto, T.; Hyon, S. H. Preparation of oriented β-form poly(L-lactic acid) by solid-state coextrusion: effect of extrusion variables. *Macromolecules* **2003**, *36*, 3601–3605.
27 Sawai, D.; Yokoyama, T.; Kanamoto, T.; Sungil, M.; Hyon, S. H.; Myasnikova, L. P. Crystal transformation and development of tensile properties upon drawing of poly(L-lactic acid) by solid-state coextrusion: effects of molecular weight. *Macromol. Symp.* **2006**, *242*, 93–103.
28 Brizzolara, D.; Cantow, H. J.; Diederichs, K.; Keller, E.; Domb, A. J. Mechanism of the stereocomplex formation between enantiomeric poly(lactide)s. *Macromolecules* **1996**, *29*, 191–197.
29 Brochu, S.; Prud'homme, R. E.; Barakat, I.; Jerome, R. Stereocomplexation and morphology of polylactides. *Macromolecules* **1995**, *28*, 5230–5239.
30 Sun, J.; Yu, H.; Zhuang X.; Chen X.; Jing X. Crystallization behavior of asymmetric PLLA/PDLA blends. *J. Phys. Chem. B* **2011**, *115*, 2864–2869.
31 Pulst, M.; Samiullah, M. H.; Baumeister, U.; Prehm, M.; Balko, J.; Thurm-Albrecht, T.; Busse, K.; Golitsyn, Y.; Reichert, D.; Kressler, J. Crystallization of poly(ethylene oxide) with a well-defined point defect in the middle of the polymer chain. *Macromolecules* **2016**, *49*, 6609–6620.
32 Huang Y.; Zhang Z.; Li Y.; Xu, J.; Xu, L.; Yan, Z.; Zhong, G.; Li, Z. The role of melt memory and template effect in complete stereocomplex crystallization and phase morphology of polylactides. *Cryst. Growth Des.* **2018**, *18*, 1613–1621.
33 Michell, R. M.; Müller, A. J. Confined crystallization of polymeric materials. *Prog. Polym. Sci.* **2016**, *54-55*, 183-213.
34 Zhang, P.; Huang, H.; He, T.; Hu, Z. Long-range ordered crystallization structure in the micromolded diblock copolymer thin film. *ACS Macro. Lett.* **2012**, *1*, 1007–1011.
35 Huang, C.; Jiao, L.; Zeng, J.; Zhang, J.; Yang, K.; Wang, Y. Fractional crystallization and homogeneous nucleation of confined PEG microdomains in PBS-PEG multiblock copolymers. *J. Phys. Chem. B* **2013**, *117*, 10665–10676.
36 Wu, B.; Yang, W.; Niu, D.; Dong, W.; Chen, M.; Liu, T.; Du, M.; Ma, P. Stereocomplexed poly(lactide) composites toward engineering plastics with superior toughness, heat resistance and anti-hydrolysis. *Chinese J. Polym. Sci.* **2020**, *38*, 1107–1116.
37 Pan, P.; Zhao, L.; Yang, J.; Inoue, Y. Fractional crystallization and phase segregation in binary miscible poly(butylene succinate)/poly(ethylene oxide) crystalline blends: effect of crystallization temperature. *Macromol. Mater. Eng.* **2013**, *298*, 201–209.
38 Pan, P.; Zhao, L.; Inoue, Y. Fractional crystallization kinetics of poly(ethylene oxide) in its blends with poly(butylene succinate): Molecular weight effects. *Macromol. Mater. Eng.* **2013**, *298*, 919–927.
39 Xie, Q.; Han, L.; Zhou, J.; Shan, G.; Bao, Y.; Pan, P. Homocrystalline mesophase formation and multistage structural transitions in stereocomplexable racemic blends of block copolymers. *Polymer* **2020**, *189*, 122180.
40 Yu, C.; Han, L.; Bao, J.; Shan, G.; Bao, Y.; Pan, P. Polymorphic crystallization and crystalline reorganization of poly(L-lactic acid)/poly(D-lactic acid) racemic mixture influenced by blending with poly(vinylidene fluoride). *J. Phys. Chem. B* **2016**, *120*, 8046–8054.
41 Hoogsteen, W.; Postema, A. R.; Pennings, A. J.; Brinke, G. T.; Zugenmaier, P. Crystal structure, conformation and morphology of solution-spun poly(L-lactide) fibers. *Macromolecules* **1990**, *23*, 634–642.
42 Lorenzo, A. T.; Arnal, M. L.; Albuerne, J.; Müller, A. J. DSC isothermal polymer crystallization kinetics measurements and the use of the Avrami equation to fit the data: Guidelines to avoid common problems. *Polym. Test.* **2007**, *26*, 222–231.
43 Li Y.; Han C. Isothermal and nonisothermal cold crystallization behaviors of asymmetric poly(L-lactide)/poly(D-lactide) blends. *Ind. Eng. Chem. Res.* **2012**, *51*, 15927–15935.
44 Tol, R. T.; Mathot, V. B. F.; Groeninckx, G. Confined crystallization phenomena in immiscible polymer blends with dispersed micro- and nanometer sized PA6 droplets, part 3: Crystallization kinetics and crystallinity of micro- and nanometer sized PA6 droplets crystallizing at high supercoolings. *Polymer* **2005**, *46*, 2955–2965.
45 Chen, L.; Jiang, J.; Wei, L.; Wang, X.; Xue, G.; Zhou, D. Confined nucleation and crystallization kinetics in lamellar crystalline-amorphous diblock copolymer poly(ε-caprolactone)-*b*-poly(4-vinylpyridine). *Macromolecules* **2015**, *48*, 1804–1812.
46 Palacios, J. K,; Zhao, J.; Hadjichristidis,N.; Müller, A. J. How the complex interplay between different blocks determines the isothermal crystallization kinetics of triple-crystalline PEO-*b*-PCL-*b*-PLLA triblock terpolymers. *Macromolecules* **2017**, *50*, 9683–9695.
47 Zhang, J.; Duan, Y.; Sato, H.; Tsuji, H.; Noda, I.; Yan, S.; Ozaki, Y. Crystal modifications and thermal behavior of poly(L-lactic acid) revealed by infrared spectroscopy. *Macromolecules* **2005**, *38*, 8012–8021.

https://doi.org/10.1007/s10118-022-2658-8